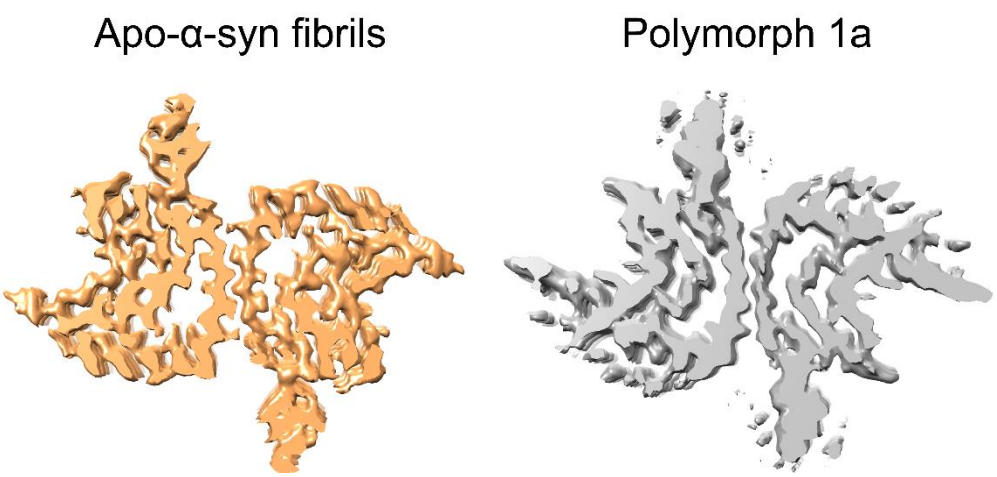


**Supplementary Figure 1. Density maps of the apo-α-syn fibril and α-syn fibril polymorph 1a.**
Cross-section view of the density maps of the apo-α-syn fibril (left) and α-syn fibril polymorph 1a (PDB ID: 6A6B, EMDB ID: EMD-6988).

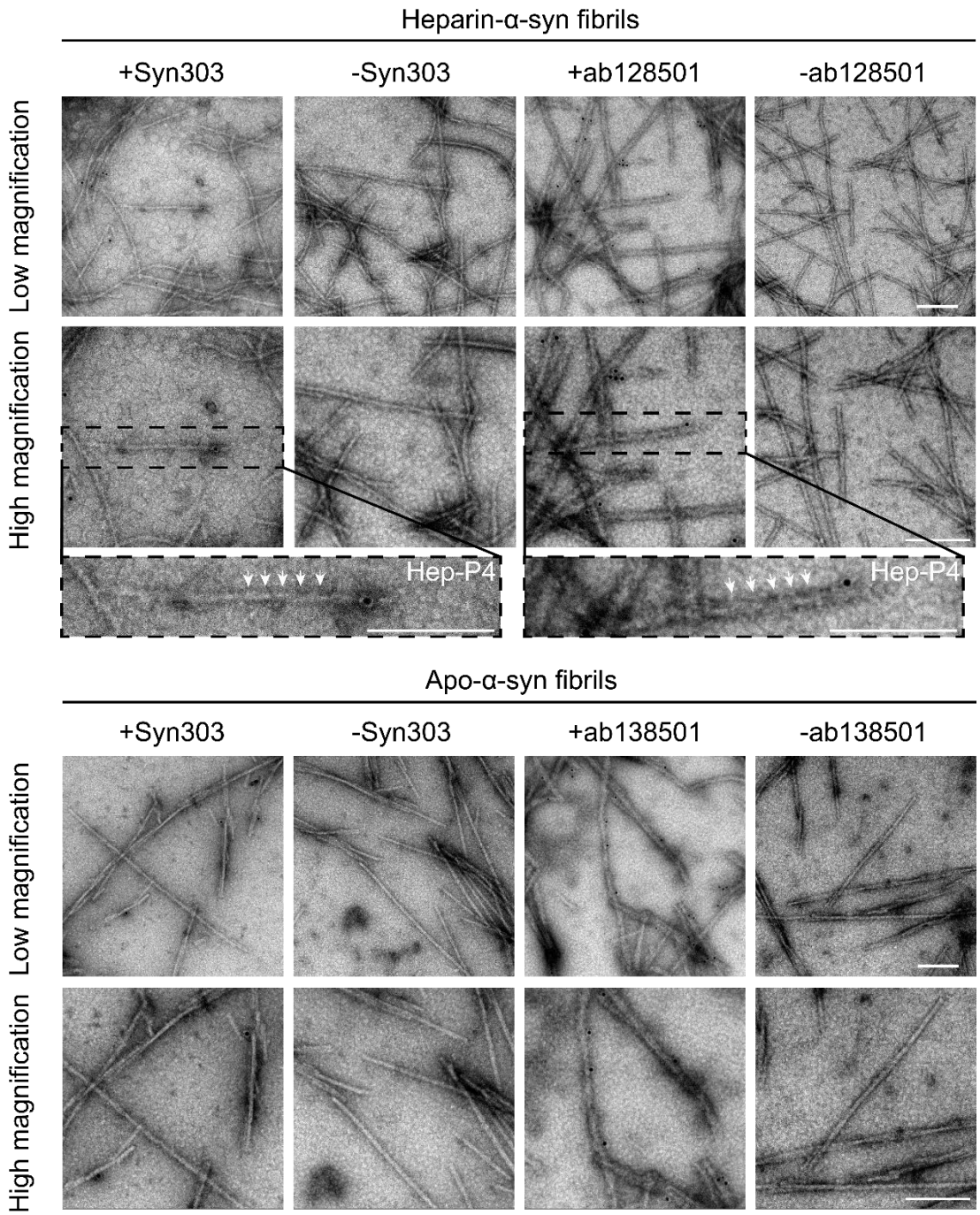


**Supplementary Figure 2. Immunoglod labeling TEM of α-syn in fibrils.**
Representative immunogold labeling TEM imaging of heparin- and apo-α-syn fibrils. The fibrils were incubated with α-syn antibodies Syn303 (recognizing residues 1-5) and ab138501 (recognizing residues 118-123) from three biologically independent experiments. Scale bar, 200 nm. Hep-P4 in the heparin-α-syn fibrils is enlarged. White arrows indicate the helical half pitches of Hep-P4.

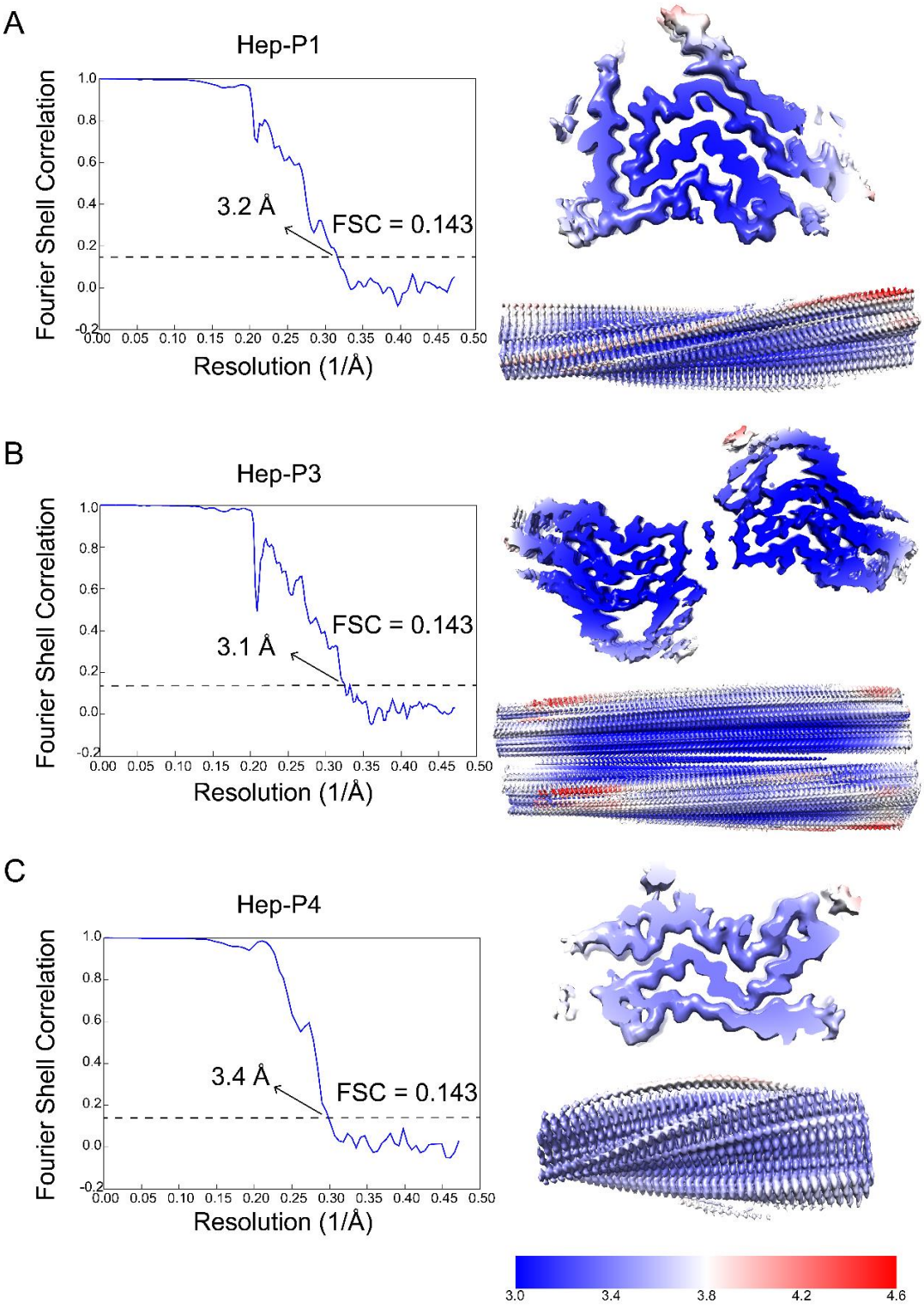


**Supplementary Figure 3. Resolution estimation of the cryo-EM structures of Hep-P1, Hep-P3 and Hep-P4.**

Left: Gold standard Fourier shell correction curves for the Hep-P1 (**A**), Hep-P3 (**B**), and Hep-P4 (**C**). The overall resolution of Hep-P1, Hep-P3, and Hep-P4 is 3.2 Å, 3.1 Å, and 3.4 Å, respectively.

Right: Local resolution estimation for the Hep-P1 (**A**), Hep-P3 (**B**), and Hep-P4 (**C**).

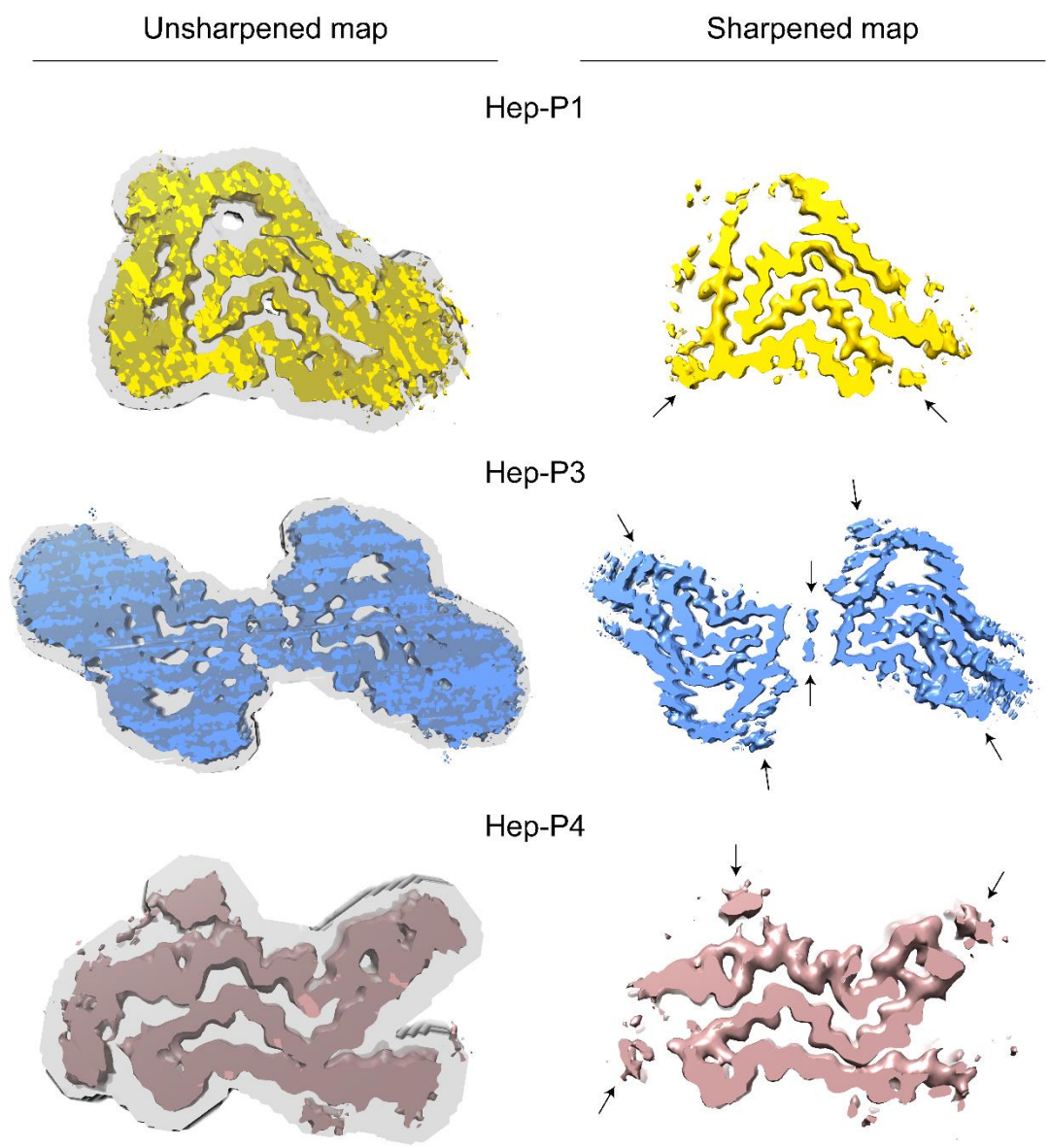


**Supplementary Figure 4. Sharpening for heparin-α-syn fibril maps.**
Unsharpened maps are shown on the left with initial binarization threshold of 0.0049 for unsharpened Hep-P1 map, 0.00214 for unsharpened Hep-P3 map, and 0.00578 for unsharpened Hep-P4 map, respectively. The masks used for post-processing are shown in gray.
After post-processing, sharpened maps are shown on the right with threshold of 0.0125 for sharpened Hep-P1 map, 0.008 for sharpened Hep-P3 map, and 0.0095 for sharpened Hep-P4 map, respectively. The extra densities corresponding to heparin are indicated by arrows.

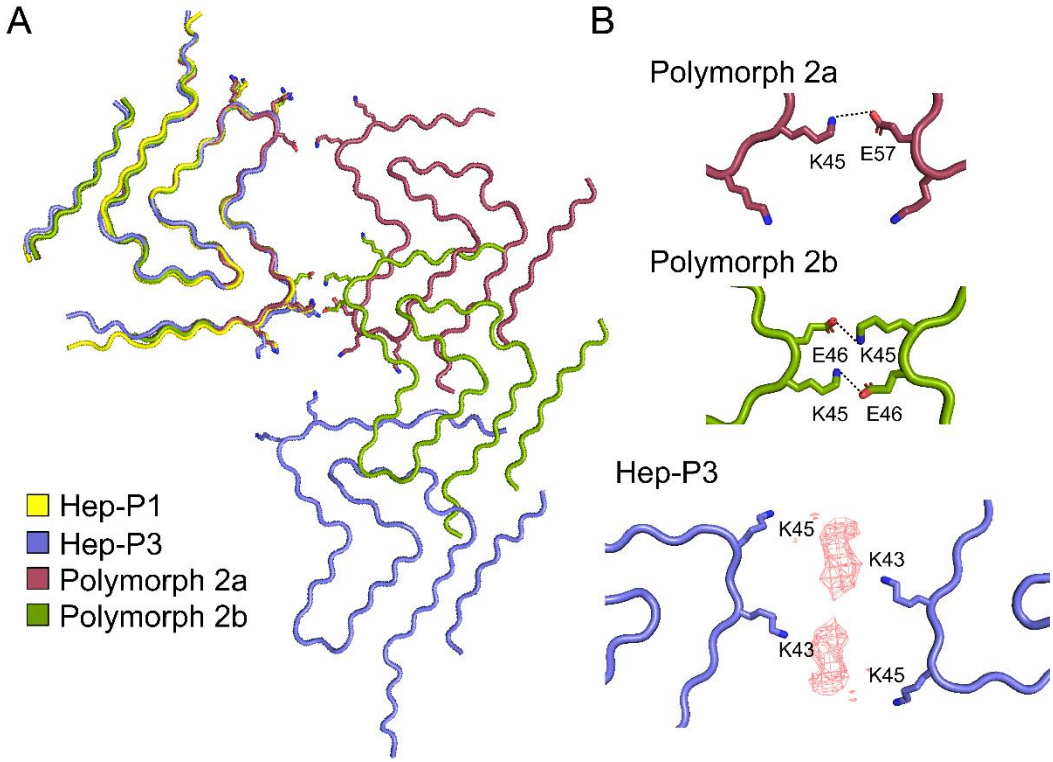


**Supplementary Figure 5. Structural comparison of Hep-P1 with Hep-P3, α-syn fibril polymorphs 2a and 2b.**

**A.** Alignment of the α-syn structures in one layer of the fibrils including Hep-P1 (yellow, monomer), Hep-P3 (blue, dimer), polymorph 2a (purple, dimer) and polymorph 2b (green, dimer). The root mean square deviations (RMSD) between Hep-P1 and Hep-P3 is 0.972 Å over 62 C-α atoms. The RMSD between Hep-P1 and polymorph 2a (PDB ID: 6SSX) is 0.961 Å over 63 C-α atoms. The RMSD between Hep-P1 and polymorph 2b (PDB ID: 6SST) is 0.688 Å over 60 C-α atoms.

**B.** Zoom-in views of the protofilamental interfaces of polymorph 2a, polymorph 2b and Hep-P3. Residues involved in the interfaces are highlighted and the side chains are shown as sticks. The pink meshes in Hep-P3 represent the densities of heparin.

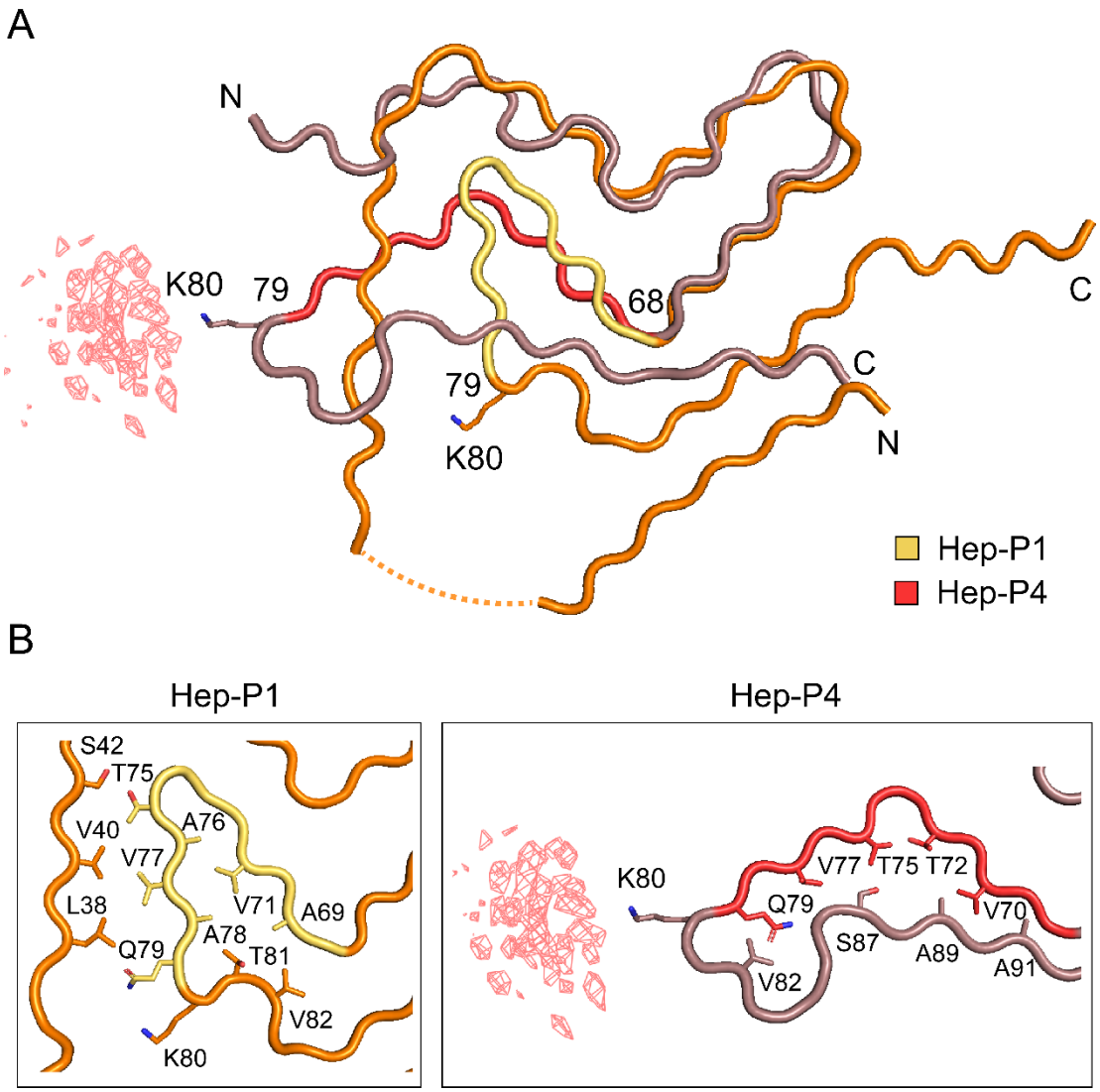


**Supplementary Figure 6. Heparin binding with K80 drives the new fold generation in Hep-P4.**

**A.** Overlay of the α-syn structures of Hep-P1 (brown) with Hep-P4 (yellow). The V-shaped structural motif formed by residues 68-79 are colored in orange (Hep-P1) and red (Hep-P4), respectively. The additional density adjacent to K80 in Hep-P4 is shown by mesh.

**B.** Zoom-in views of the local conformation of the V-shaped structural motif in Hep-P1 (left) and Hep-P4 (right). The side chains are shown as sticks.

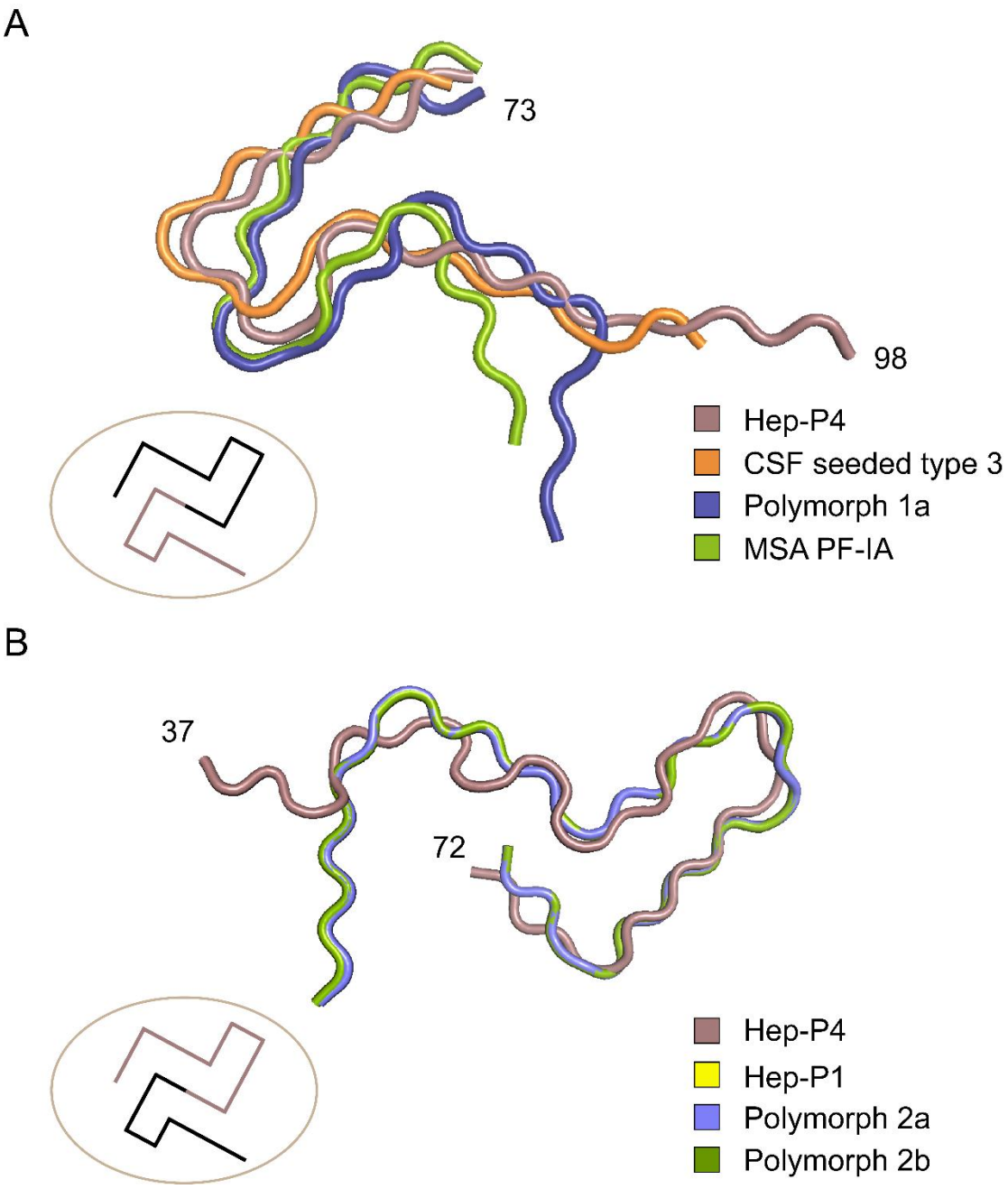


**Supplementary Figure 7. Hep-P4 is a hybrid structure of two common α-syn structural motifs.**

**A.** Structural comparison of the C-terminal half (residue 73-98) of Hep-P4 with CSF seeded type 3 polymorph (PDB ID: 7V49, RMSD 2.766 Å over 22 C-α atoms), polymorph 1a (PDB ID: 6A6B, RMSD 3.506 Å over 22 C-α atoms), and MSA PF-IA (PDB ID: 6XYO, RMSD 2.942 Å over 22 C-α atoms).

**B.** Structural comparison of the N-terminal half (residue 37-72) of Hep-P4 with Hep-P1 (RMSD 2.911 Å over 32 C-α atoms), polymorph 2a (PDB ID: 6SSX, RMSD 2.882 Å over 32 C-α atoms), and polymorph 2b (PDB ID: 6SST, RMSD 2.864 Å over 32 C-α atoms).

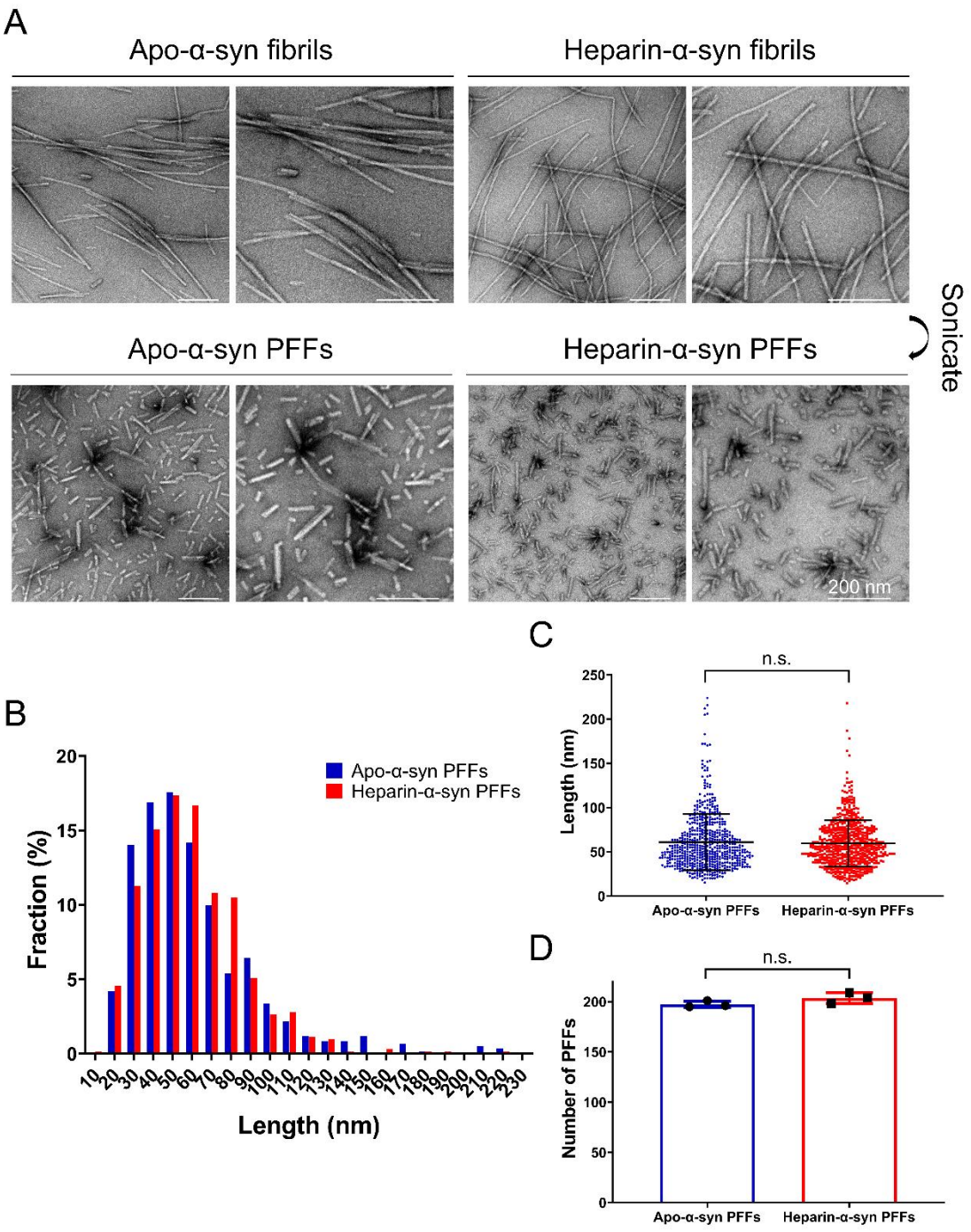


**Supplementary Figure 8. Characterization and quantification of apo-α-syn PFFs and heparin-α-syn PFFs used in the cell assay.**

**A.** Representative negative-staining TEM images of the apo-α-syn and the heparin-α-syn fibrils (top) and PFFs after sonication (bottom) from three biologically independent experiments. Images are shown with two magnifications for each sample. Scale bars are 200 nm.

**B.** Size distribution of apo-α-syn PFFs (592 particles) and heparin-α-syn fibrils PFFs (611 particles). The percentages for PFFs length were analyzed with Frequency distribution in GraphPad Prism 8.

**C.** PFFs length of apo-α-syn PFFs (592 particles) and heparin-α-syn PFFs (611

particles). Data are shown as mean ± s.d. The length of PFFs were measured from 3 independent reproducible TEM images. P=0.3723, unpaired, two-tailed Student's t test. **D.** Amounts of apo-α-syn PFFs and heparin-α-syn PFFs. The amounts were counted in 3 independent reproducible TEM images and shown as mean ± s.d. P=0.1605, unpaired, two-tailed Student's t test.

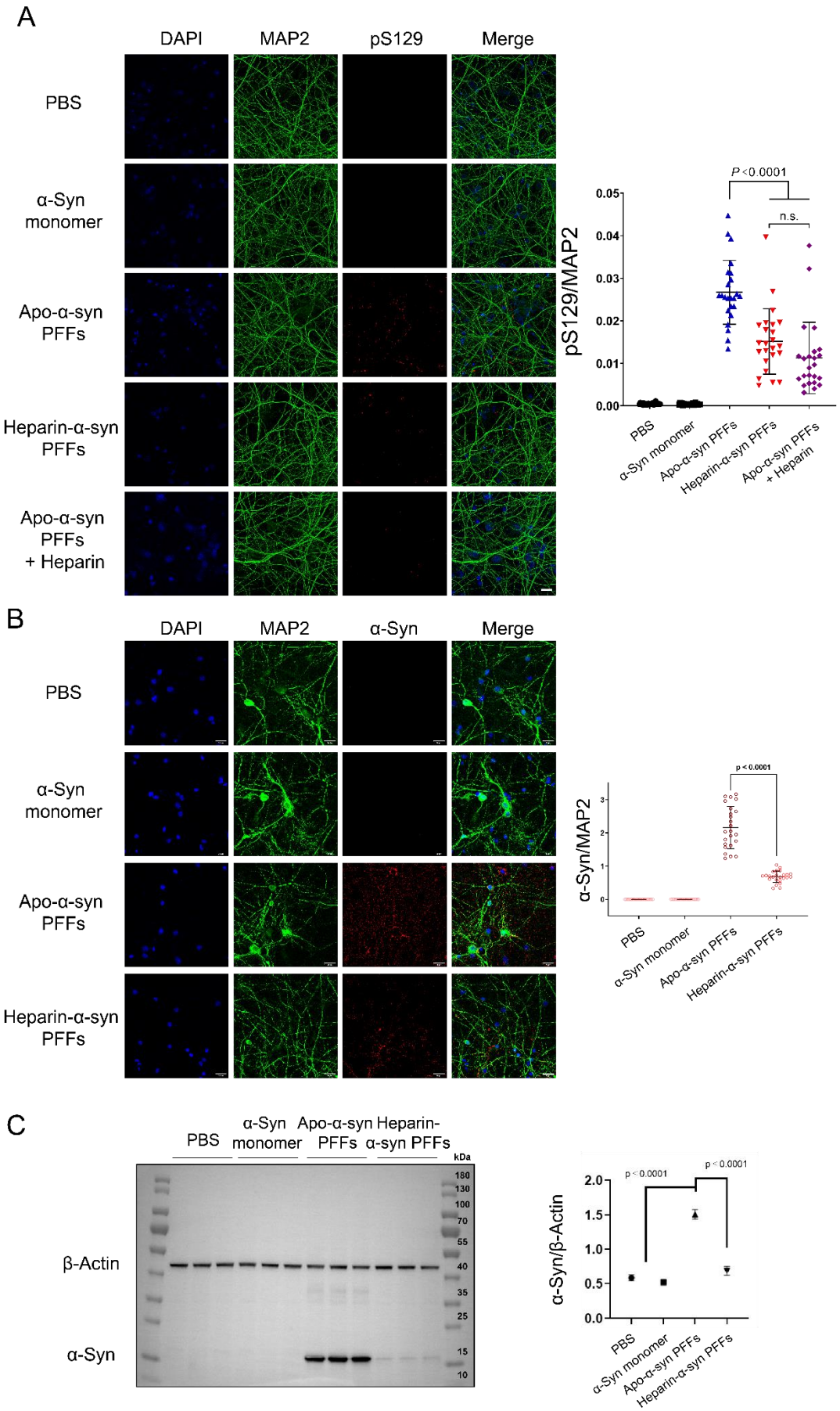
A
DAPI
MAP2
pS129
Merge
PBS
α-Syn monomer
Apo-α-syn PFFs
Heparin-α-syn PFFs
Apo-α-syn PFFs + Heparin
P<0.0001
n.s.
pS129/MAP2
0.05
0.04
0.03
0.02
0.01
0.00
PBS
α-Syn monomer
Apo-α-syn PFFs
Heparin-α-syn PFFs
Apo-α-syn PFFs + Heparin
B
DAPI
MAP2
α-Syn
Merge
PBS
α-Syn monomer
Apo-α-syn PFFs
Heparin-α-syn PFFs
p < 0.0001
α-Syn/MAP2
3
2
1
0
PBS
α-Syn monomer
Apo-α-syn PFFs
Heparin-α-syn PFFs
C
PBS
α-Syn monomer
Apo-α-syn PFFs
Heparin-α-syn PFFs
kDa
180
130
100
70
55
40
35
25
15
10
β-Actin
α-Syn
p < 0.0001
p < 0.0001
α-Syn/β-Actin
2.0
1.5
1.0
0.5
0.0
PBS
α-Syn monomer
Apo-α-syn PFFs
Heparin-α-syn PFFs

**Supplementary Figure 9. Heparin-α-syn complex fibrils show attenuated neuropathology.**

**A.** Left: Representative immunofluorescence images of rat primary cortical neurons treated with PBS, 200 nM α-syn monomer, 200 nM apo-α-syn PFFs, 200 nM heparin-α-syn PFFs, and 200 nM apo-α-syn PFFs + 2.4 μg $ml^{-1}$ heparin (comparable amount of heparin with that in heparin-α-syn PFFs, mixed in medium). The fixed neurons were immunostained for DAPI (blue), MAP2 (green), phosphorylated S129 α-syn (pS129, red). Scale bar, 20 μm. Right: Quantification of the pS129 intensity normalized to MAP2 intensity. Data are shown as mean ± SD of 24 images in three independent experiments. Statistical significance was measured using one-way ANOVA followed by Tukey's post-hoc test. There was no significance between heparin-α-syn PFFs group and apo-α-syn PFFs+heparin group (P=0.1835).

**B.** Left: Representative immunofluorescence images of the α-syn surface binding on rat primary cortical neurons treated with PBS, α-syn monomer, apo-α-syn PFFs and hep-α-syn PFFs. The fixed neurons were immunostained for DAPI (blue), MAP2 (green), α-syn (red). The α-syn antibody (ab138501) specifically recognizes human α-syn. Scale bar, 20 μm. Right: Quantification of the bound α-syn intensity normalized to MAP2 intensity. Data are shown as mean ± SD of 24 images in three independent experiments. Statistical significance was measured using one-way ANOVA followed by Tukey's post-hoc test.

**C.** Western blot of the α-syn that were taken up by primary cortical neurons. The α-syn antibody (ab138501) specifically recognizes human α-syn. β-Actin was used as a loading control. The cellular uptake of α-syn were quantitated by measuring the intensity of bands normalized to β-actin intensity. Data are means ± SD of three independent experiment samples. Statistical significance was measured using one-way ANOVA followed by Tukey's post-hoc test.

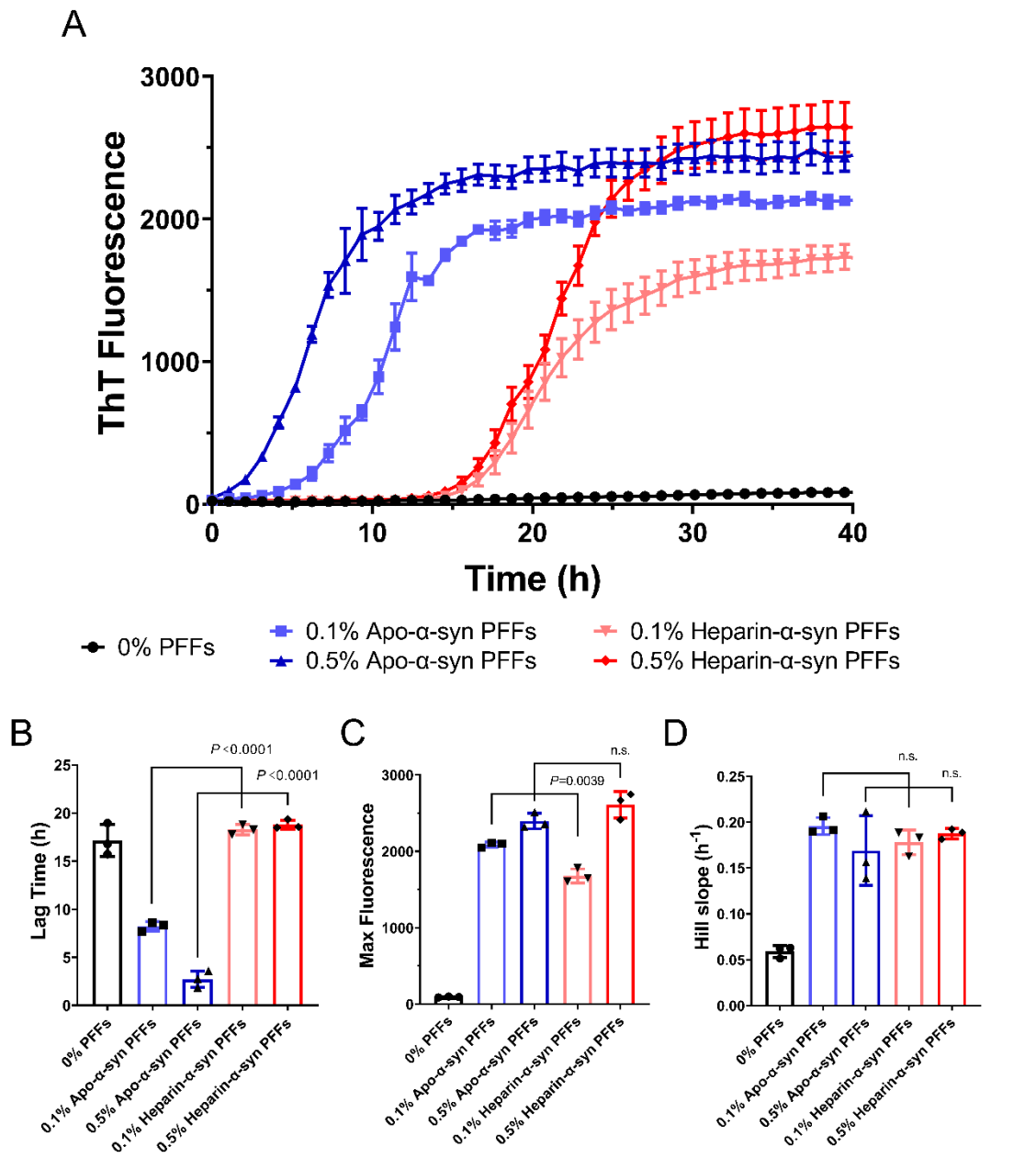


**Supplementary Figure 10. Seeding properties of the apo-α-syn PFFs and heparin-α-syn PFFs.**

**A. ThT assay for** α-syn alone (colored in black) or in the presence of 0.1 mol% apo-α-syn PFFs (colored in light blue), 0.5 mol% apo-α-syn PFFs (colored in dark blue), 0.1 mol% heparin-α-syn PFFs (colored in light red), and 0.5 mol% heparin-α-syn PFFs (colored in dark red), respectively. Data are shown as mean ± s.d., n = 3 independent samples.

**B.** The lag time of apo-α-syn PFFs seeded aggregation and heparin-α-syn PFFs seeded aggregation. Data are shown as mean ± s.d., n = 3 independent samples. Statistical significance was measured using one-way ANOVA followed by Tukey's post-hoc test.

**C.** The max fluorescence intensity of apo-α-syn PFFs seeded aggregation and heparin-α-syn PFFs seeded aggregation. Data are shown as mean ± s.d., n = 3 independent samples. Statistical significance was measured using one-way ANOVA followed by

Tukey's post-hoc test. There was no significance between 0.5 mol% apo-α-syn PFFs and 0.5 mol% heparin-α-syn PFFs group (P=0.1476).

**D.** The hill slope of apo-α-syn PFFs seeded aggregation and heparin-α-syn PFFs seeded aggregation. Data are shown as mean ± s.d., n = 3 independent samples. Statistical significance was measured using one-way ANOVA followed by Tukey's post-hoc test. There was no significance between apo-α-syn PFFs and heparin-α-syn PFFs group (P=0.7799 for 0.1 mol% seeds comparison, P=0.7484 for 0.5 mol% seeds comparison).

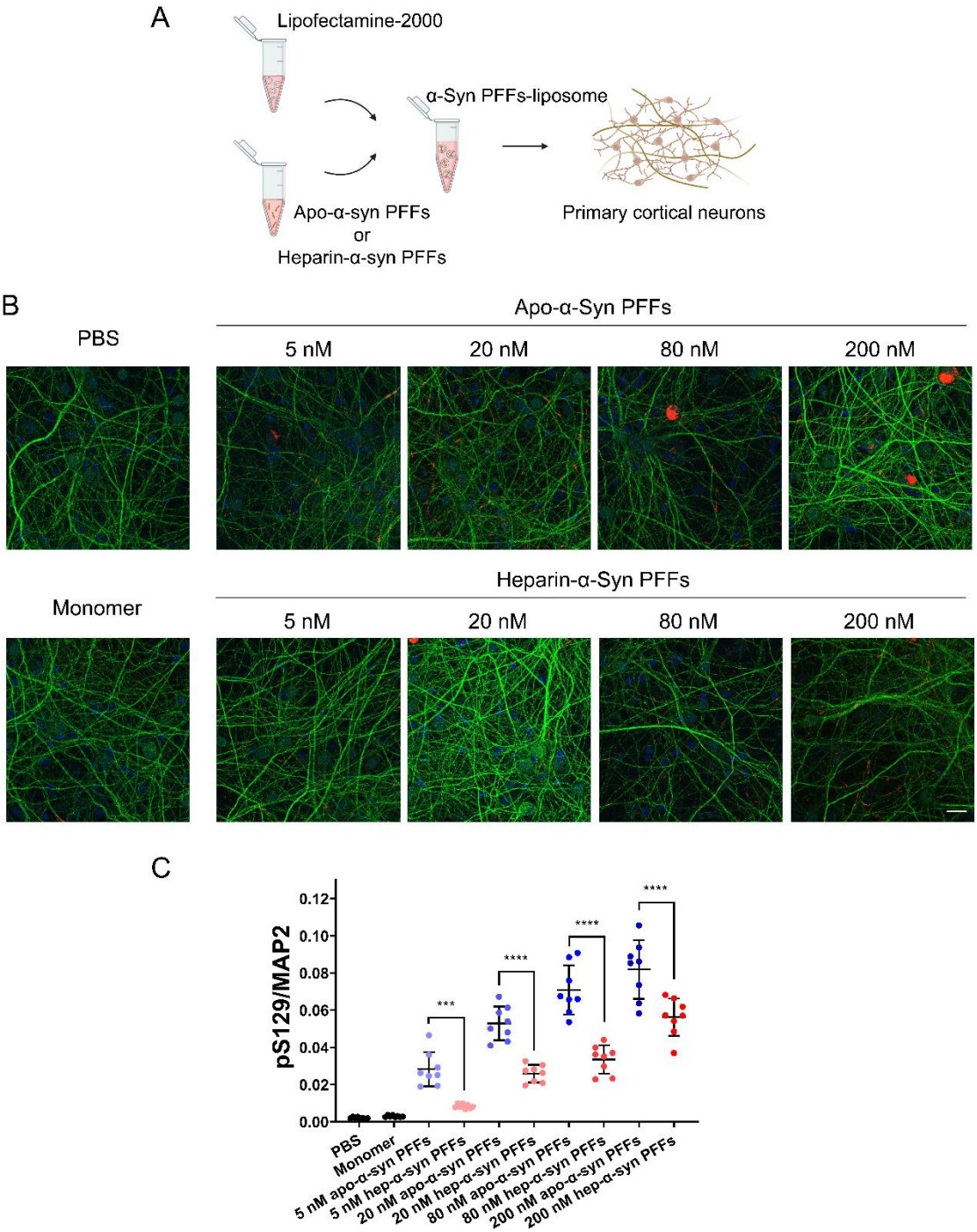


**Supplementary Figure 11. Seeding capacity of apo-α-syn PFFs and heparin-α-syn PFFs to endogenous α-syn in primary neuron.**

**A.** Schematic diagram of the liposome mediated seeds transduction process. The figure is created with BioRender.com.

**B.** Representative immunofluorescence images of rat primary cortical neurons treated with liposome with PBS, α-syn monomer, apo-α-syn PFFs (5, 20, 80, 200 nM), heparin-α-syn PFFs (5, 20, 80, 200 nM). The fixed neurons were immunostained for DAPI (blue), MAP2 (green), phosphorylated S129 α-syn (pS129, red).

**C.** Quantification of the pS129 intensity normalized to MAP2 intensity. Data are shown

as mean ± SD of 8 images in three independent experiments. Statistical significance was measured using one-way ANOVA followed by Tukey's post-hoc test. ***P=0.0009; ****P < 0.0001.